Supplementary Materials for

Widespread post-transcriptional regulation of co-transmission

Yunpeng Zhang[1†], Nannan Chen[1†], Emmanuel J. Rivera-Rodriguez[1†], Albert D. Yu[1,2], Michael Hobin[1], Michael Rosbash[1,2] and Leslie C. Griffith[1*]

Correspondence to: griffith@brandeis.edu

This PDF file includes:

Materials and Methods

Fly strains and husbandry

All flies were raised on standard food at 25 ℃ with a 12h:12h light-dark cycle, except for the *Tubulin-Gal80^{ts}* experiments to induce expression at different developmental stages, where flies were raised at either 18 ℃ or 29 ℃. Male and female flies were collected at eclosion and aged as specified before performing experiments. *VT030559-GAL4* was obtained from Vienna Drosophila Resource Center (VDRC) stock center. *VAChT$^{[MI08244]}$* (#55439), *nsyb-Gal4* (#51941), *VGluT-Gal4* (#60312), *VGluT-p65-AD* (#82986), *VGluT-GAL4-DBD* (#60313), *ChAT-Gal4* (#60317), *GH146-Gal4* (#30026), *GMR81C04-Gal4* (#48378), *VGAT-Gal4* (#84696), *UAS-miR-190-sponge* (#61397), *UAS-scramble-sponge* (#61501), *UAS-Flp* (#4539), *UAS-CD4-GFP$^{1-10}$* (#93016), *VGluT-Gal80* (#58448) and *tubulin-Gal80^{ts}* (#7016) were obtained from Bloomington *Drosophila* stock center. *UAS-myrGFP-2A–RedStinger (27)* was obtained from the Ganetzky lab at University of Wisconsin, and *UAS-UNC84::GFP* from Gilbert Henry at Janelia Research Campus.

Generation of *EGFP::VAChT*, *RFP::VGluT* and *RFP::VGAT* lines

To knock in *EGFP* at the N-terminal of *VAChT*, we designed a guide RNA which recognized the beginning of *VAChT* with an online tool (http://targetfinder.flycrispr.neuro.brown.edu/) and created a donor plasmid (pMC1-EGFP-VAChT plasmid in Data S1). The guide RNA was cloned into a pU6 plasmid (Addgene, #45946) and injected into Cas9 flies (*y,sc,v; nos-Cas9/CyO;* +/+) with the donor plasmid. By the same strategy, we knocked in *RFP* at the N-terminal of *VGluT* and *VGAT*. All guide RNAs are listed in Table S1 and donor plasmids are shown in Data S1. Correct integrations were confirmed by PCR and sequencing with primers which bind outside the regions of the integrated junction.

Creation of *Frt-stop-Frt-ECFP::VAChT*, *Frt-stop-Frt-EGFP::VGluT* and *Frt-stop-Frt-EGFP::VGAT* flies

For the *Frt-stop-Frt-ECFP::VAChT* fly strain, we used the same guide RNA as *EGFP::VAChT* and made a donor plasmid (pMC10-Frt-stop-3p3-RFP-Frt-ECFP::VAChT plasmid in Data S1). We amplified the stop sequence which was flanked by two Frt sites, *ECFP* sequence, and *VAChT* sequence. 3P3 RFP sequence was amplified and inserted between stop and the second Frt site for screening. These fragments were assembled in order and cloned into the pMC10 plasmid. The guide RNA was cloned into pU6 plasmids and injected into Cas9 flies with the donor plasmid. F1 progeny with RFP markers were selected as candidates, and further confirmation was performed by PCR and sequencing. By the same strategy, we made *Frt-stop-Frt-EGFP::VGluT* and *Frt-stop-Frt-EGFP::VGAT* flies. The guide RNAs are listed in Table S1, and the donor plasmids were shown as pMC10-Frt-stop-3P3-RFP-Frt-EGFP::VGluT and pMC10-Frt-stop-3P3-RFP-Frt-EGFP::VGAT in Data S1.

Creation of *Flp-VAChT-3'UTR* flies

For the *Flp-VAChT-3'UTR* fly strain, we used the same guide RNA as *EGFP::VAChT* and made a donor plasmid (pMC10-Flp-VAChT-3'UTR plasmid in Data S1). The guide RNA was cloned into the pU6 plasmid and injected into Cas9 flies with the donor plasmid. Correct integrations were confirmed by PCR and sequencing.

Creation of split-Gal4 lines

To make the *VAChT-AD* and *VAChT-DBD* fly strains, the phase 0 T2A-p65AD-Hsp70 plasmid (Addgene, #62914) and T2A-Gal4DBD-Hsp70 plasmid (Addgene, #62903) were injected into $VAChT^{[MI08244]}$ flies with pBS130 plasmid (Addgene, #26290) which encodes phiC31 integrase. Progeny were crossed to *yw* flies to check for spGAL4 insertion. Male flies with yellow marker

were selected as candidates, and then checked by PCR to obtain insertion lines in the correct orientation.

For the *VGAT-AD* and *VGAT-DBD* lines, we first made a *3P3-RFP-VGAT* fly strain utilizing the same guide RNA as *RFP::VGAT* (Table S1) and a donor plasmid which contained attp flanked *3P3-RFP* sequences (Fig. S1A). Flies were first screened for RFP expression, and then confirmed by PCR and sequencing. To make *VGAT-AD* flies, the AD sequence was amplified from T2A-p65AD-Hsp70 plasmid (Addgene, #62914) and attached at the N terminal of the VGAT sequence. The whole AD sequence which was flanked by two inverted-attB sites was cloned into the pBS-KS-attB2 plasmid (Addgene, #62897). This plasmid was injected into *3P3-RFP-VGAT* flies, with plasmids that expressed phiC31 recombinase. By the same strategy, we made *VGAT-DBD* flies using T2A-Gal4DBD-Hsp70 plasmid (Addgene, #62903). F1 progeny without RFP marker were selected as candidates, and further confirmation by PCR and sequencing were performed.

Creation of *VAChT-GFP$^{1-10}$*, *VAChT-GFP^{11}*, and *VGAT-GFP^{11}* lines

To make the *VAChT-GFP$^{1-10}$* and *VAChT-GFP^{11}* fly strains, we first chosen a luminal-side insertion site using *in silico* prediction (https://phobius.sbc.su.se/). We used the same guide RNA as *EGFP::VAChT*, and created donor plasmids (VAChT-GFP1-10 plasmid and VAChT-GFP11 plasmid in Data S1). The guide RNA was cloned into a pU6 plasmid and injected into Cas9 flies with the donor plasmids. Correct integrations were confirmed by PCR and sequencing.

For the *VGAT-GFP^{11}* line, a luminal-side insertion site was chosen using *in silico* prediction (https://phobius.sbc.su.se/). The GFP^{11} sequence was inserted at the last luminal side site of the VGAT. The whole sequence was flanked by two inverted-attB sites, and cloned into the pBS-KS-attB2 plasmid (Addgene, #62897). This plasmid (VGAT-GFP11 plasmid in Data S1) was injected into *3P3-RFP-VGAT* flies showed above, with plasmids that expressed phiC31

recombinase. F1 progeny without RFP marker were selected as candidates, and further confirmation by PCR and sequencing were performed. Luminal location of the tags was confirmed as shown in Fig. S11.

Creation of *UAS-ChAT, UAS-VAChT, UAS-Fluc-ChAT 3'UTR* and *UAS-Fluc-ChAT del* lines

For the *UAS-RFP::ChAT* fly strain, the coding region of ChAT was amplified from a *Canton-S* wild type fly cDNA library, and inserted into the pUAST-attB plasmid (Addgene, 8489bp) using the Gibson assembly method (UAS-RFP::ChAT plasmid in Data S1). To allow visualization of ChAT expression, RFP was inserted in-frame before the ChAT coding region. Using the same strategy, GFP1-10 and VAChT coding regions were amplified and inserted into pUAST-attB to make the *UAS- VAChT* fly line (UAS- GFP1-10::VAChT plasmid in Data S1).

For the *UAS-Fluc-ChAT 3'UTR* fly line, we amplified the Fluc sequence from the Ac/Fluc plasmid (a gift of Ravi Allada) and the ChAT 3'UTR sequence from the *Canton-S* wild type fly genome. These sequences were assembled in order and cloned into the pUAST-attB plasmid (UAS-Fluc-ChAT 3'UTR plasmid in Data S1). For the *UAS-Fluc-ChAT del* fly line, the same sequences were used, except that the predicted miR-190 binding sites were removed from ChAT 3'UTR (UAS-Fluc-ChAT del plasmid in Data S1).

All plasmids were checked by sequencing. UAS-RFP::ChAT, UAS-Fluc-ChAT 3'UTR and UAS-Fluc-ChAT del plasmids were injected into *phiC31-attP* flies (Bloomington Stock Center #79604) which have an attP site on the second chromosome to allow targeted integration. UAS-GFP1-10::VAChT plasmid was injected into *phiC31-attP* flies (Bloomington Stock Center #8622), which have an attP site on the third chromosome. The progeny of injected flies was screened for w^+ red eye marker, and then checked by PCR and sequencing.

INTACT purification of nuclei

Nuclei from *Glu^{ACh}>UNC84::GFP* and *GABA^{ACh}>UNC84::GFP* heads were prepared according to the INTACT protocol (*13*), with some adjustments. Briefly, whole flies were flash frozen on dry ice in 15 ml tubes and vortexed for 5 cycles of 15 s vortexing at max speed and 1 min of resting on dry ice. Heads were separated from bodies using frozen No.40 and No.25 brass sieves. Sieved heads were placed in pre-chilled 1 ml dounce homogenizers and homogenized using a modified INTACT lysis buffer (10mM Tris-HCl pH7.5, 2mM MgCl2, 10mM KCl, 0.6mM Spermidine, 0.2mM Spermine, 1mM DTT, 0.03% Tween-20, 1% BSA, 1x cOmplete Protease inhibitor), for 15 strokes with Pestle A and 15 strokes of Pestle B. Homogenized lysate was filtered through a 20 µm CellTrics Filter (Sysmex Flow Cytometry), centrifuged for 5 min at 800 RCF. Supernatant was removed and lysate was resuspended in modified INTACT lysis buffer and filtered through a 10 µm CellTrics Filter (Sysmex Flow Cytometry). Filtered lysate was then subject to anti-GFP immunoprecipitation and RNA extraction as previously described (*13*).

RNA-seq and data analysis

Purified RNA was subject to PolyA enrichment using the Poly(A)Purist Mag Kit (Thermofisher) according to protocol. Purified Poly(A) RNA was quantified using the Qubit 2.0 RNA HS Assay (Thermofisher), and 10 ng of RNA per sample was used for library prep using the NextFlex Rapid Directional qRNA-Seq Kit 2.0 (PerkinElmer) and sequenced on a NextSeq 550 using the 75 cycle High Output Kit (Illumina).

UMIs were extracted and appended to reads from sequenced libraries using umI_tools extract with the following parameters: --bc-pattern=NNNNNNNNN --bc-pattern2=NNNNNNNNN. Processed reads were then aligned against the dm6 reference genome with STAR using the following parameters: --outFilterMismatchNoverLmax 0.05 --outFilterMatchNmin 15 –outFilterMultimap Nmax 1 --outSJfilterReads Unique --alignMatesGapMax 25000. Aligned reads were converted to BAM files and sorted using samtools, and were deduplicated using

umi_tools dedup. Reads were counted using featurecounts, and normalization and differential expression was conducted using Deseq2.

The full data set is available at NCBI; GEO accession number GSE221859

Immunohistochemistry and image processing

For dissection and staining of adult fly brains, the protocol from Janelia (https://www.janelia.org/project-team/flylight/ protocols) was used. Briefly, brains were dissected in S2 solution, and then fixed in 2% PFA solution for 55 min at room temperature (RT). Then the samples were washed 4x10 mins by 0.5% PBST solution, and blocked with 5% goat serum in PBST solution for 1.5 hours. After that, the samples were incubated in primary antibody solutions for 4 hours at RT and continued incubation at 4℃ for over two nights. Then samples were washed 3x30 min by 0.5%PBST, incubated in secondary antibody solutions for 4 hours at RT, with continued incubation at 4℃ for over three nights. The same washing protocol was performed after secondary antibody incubation, then fixed by 4% PFA again for 4h at RT and mounted in Vectashield mounting medium (Vector Laboratories).

The primary antibodies used were: rabbit anti-RFP (1:200, Takara)，rabbit anti-GFP (1:1000, Thermo Fisher), mouse anti-GFP (1:200, Sigma), mouse anti-Brp (1:100, DSHB), anti-VGluT(*28*) (1:200, generous gift from Aaron DiAntonio, Washington University) and anti-VGAT (*29*) (1:200, generous gift from David Krantz, UCLA). Alexa Fluor 488 anti-mouse/rabbit antibody (Invitrogen) and Alexa Fluor 635 anti-mouse/rabbit antibody (Invitrogen) were used as secondary antibodies at 1:200 dilutions.

All images were taken using Leica SP5 confocal microscope under 20x or 60x objective lens. Then the pictures are processed and analyzed using ImageJ Fiji software(*30*).

Sleep and locomotor activity

Individual 3-5 day old male flies were loaded into 65mm x 5mm glass tubes (Trikinetics, Waltham, MA) using CO_2 anesthesia. One end of the tube is food containing 5% agarose and 2% sucrose, the other side is a cotton ball to cover it. The flies were entrained under standard 12:12 light-dark conditions for 2 days prior to data collection.

Locomotor activity was collected with the *Drosophila* Activity Monitoring System (Trikinetics) as previously described (*31*). Sleep is defined as consecutive inactivity for five or more minutes (*32*). All sleep parameters, including total sleep duration, number of sleep episodes and mean episode duration were analyzed using an Matlab program described previously (*31*) and averaged across 4 days. Statistical analysis was performed with GraphPad Prism. For all sleep parameters a D'Agostino & Pearson test was used to determine normality of data. If data were normally distributed they were analyzed using a Student T-test or ANOVA followed by Tukey test for multiple comparisons (depending on the number of groups). If data were not normally distributed they were analyzed using a Mann-Whitney or Kruskal-Wallis test followed by Dunn's test for multiple comparisons.

S2 cell assay (*33*)

S2 cells in 12-well plates were cotransfected with 15 ng of Ac/Fluc (or its derivatives), 15 ng of Ac/Rluc, and 270 ng of Ac/miR-190 or Ac/scramble by Effectene transfection reagent (Qiagen). Ac/Fluc derivatives included Fluc with ChAT-3'UTR, Fluc with VAChT-3'UTR, and Fluc with ChAT-3'UTR with the three predicted miR-190 binding sites removed. The primers are listed in Table S2. Cells were harvested 48 hours after transfection and a dual luciferase assay was performed (Promega).

***In vivo* Luciferase assays**

15 male fly brains were collected for each sample, then homogenized in 100 µl Promega Glo Lysis Buffer (Promega, Cat# E2510) at room temperature. Homogenized samples were

incubated for 10 min at room temperature, and then centrifuged for 5 min to pellet the brain remains. 50 µl of supernatant was transferred to an Eppendorf tube on ice, and another 450 µl lysis buffer was added. A multichannel pipette was used to transfer 20 µl of each sample to a white-walled 96-well plate (Costar), then 20 µl Promega Luciferase Reagent (Promega, Cat# E2510) was added to each well. The plate was incubated in dark for 10 min. Luminescence was measured on a Luminometer plate reader (Promega, Cat# GM3000).

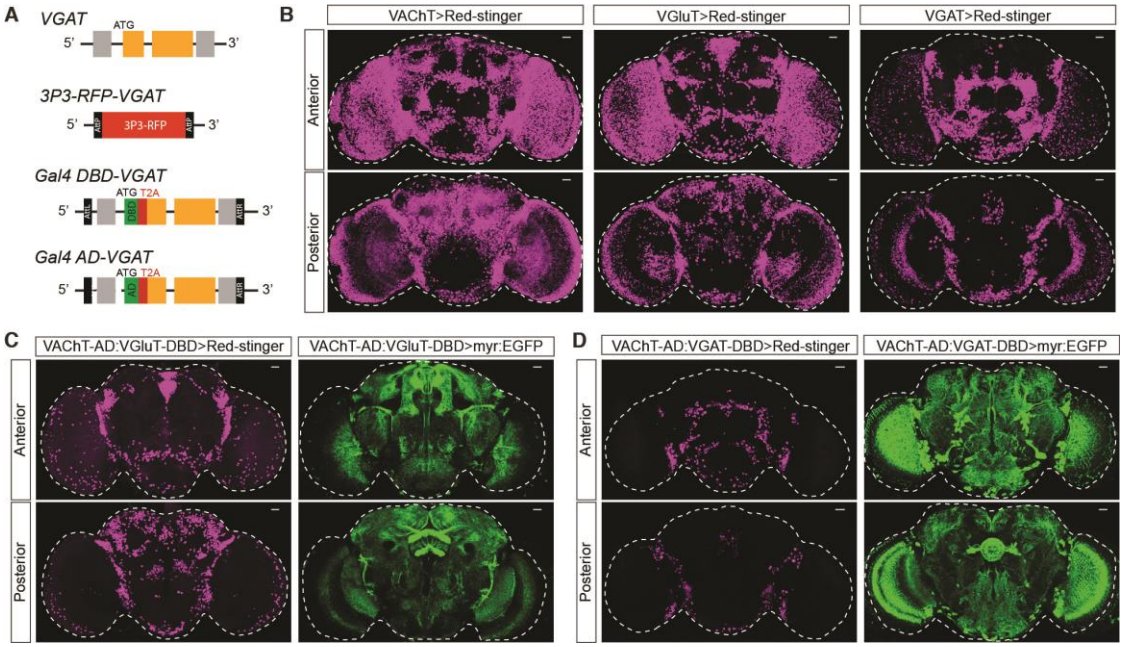

Figure S1. Expression patterns of *VAChT:VGluT* and *VAChT:VGAT* split Gal4s. (**A**) Schematic diagram showing fused *Gal4-DBD* and *Gal4-AD* knock-in strategy: attp-flanked 3P3-RFP was knocked in to replace the whole *VGAT* gene using CRISPR/Cas9. This cassette was then is replaced by attb-DBD-T2A-*VGAT*-attb or attb-AD-T2A-*VGAT*-attb using *phiC31* recombination. Grey bars indicate the UTRs, while yellow bars indicate exons. (**B**) Magenta shows the soma (nuclei) of *VAChT-Gal4, VGluT-Gal4* and *VGAT-Gal4* expression patterns: anterior views (top) and posterior (bottom). (**C-D**) Magenta shows the somatic regions of *VAChT-AD:VGluT-DBD* split-Gal4 (**C**) and *VAChT-AD:VGAT-DBD* split-Gal4 (**D**) flies, while green shows the neuronal projection regions. Dashed white lines indicate the whole brain outline. Scale bars = 20 μm for each panel. Comparison of the number of cells in B vs C/D shows that the split-GAL4s represent only a subset of the neurons captured by the broader drivers.

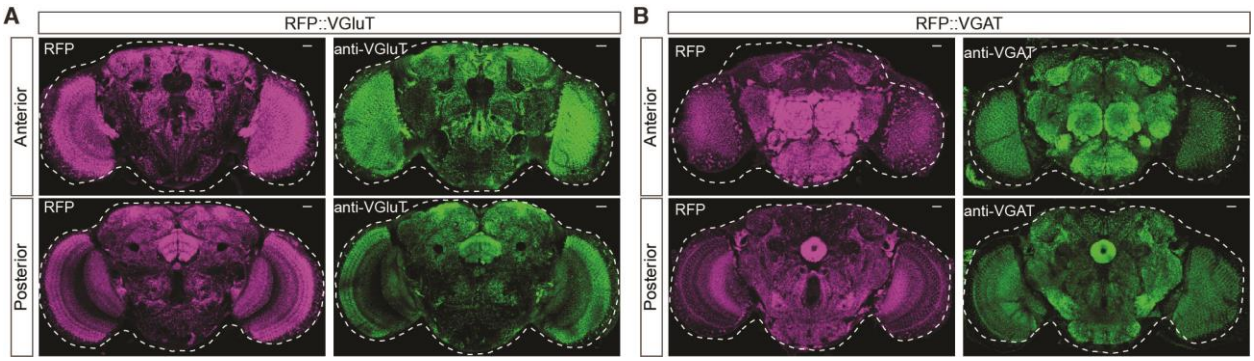

Figure S2. Validation of fusion alleles. To validate the expression patterns of our tagged vNTs, we stained heterozygous animals which have one FP-tagged allele and one untagged allele with anti-VGAT or anti-VGluT. RFP::VGluT protein from our fusion allele overlaps with wildtype chromosome VGluT staining in *RFP::VGluT/+* animals (**A**). RFP::VGAT protein overlaps with wild type chromosome VGAT staining in *RFP::VGAT/+* animals (**B**). Anterior (top) and posterior (down) pictures are shown separately. Scale bars = 20 μm for each panel.

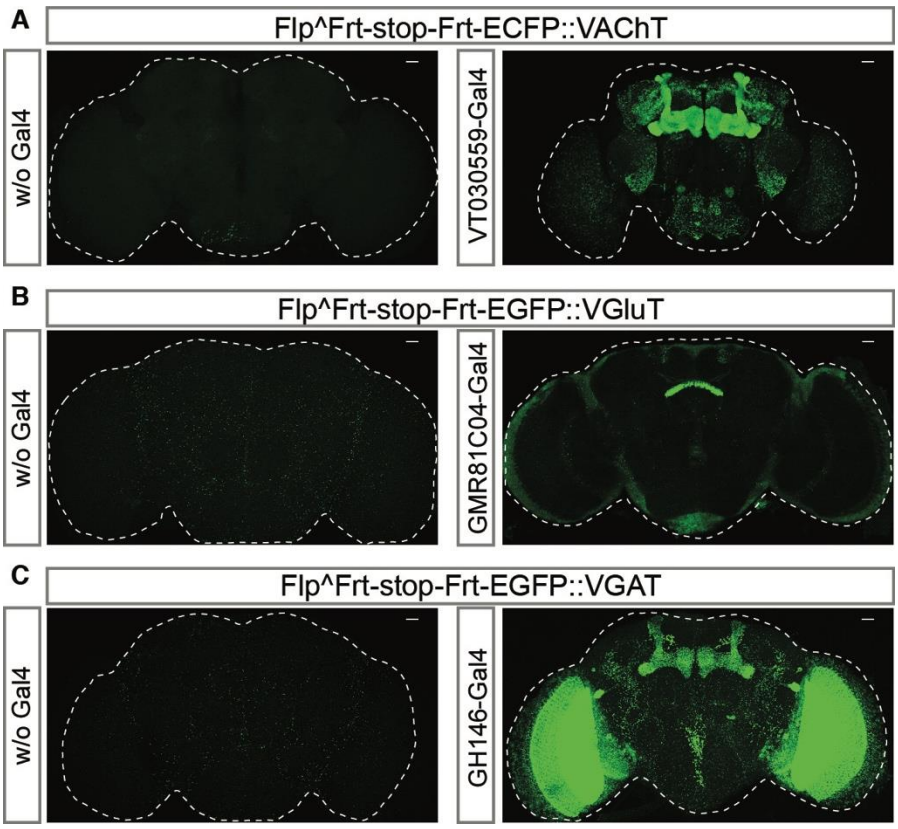

Figure S3. Validation of conditional vNT::FP fusion alleles. Gal-4 drivers for brain regions known to contain neurons expressing a particular neurotransmitter system were used to validate our flip-out strategy. (**A**) *VT030559-Gal4* driving FLP recombinase allows expression of ECFP::VAChT in the mushroom body Kenyon cells, which are known to be cholinergic. No ECFP signal is present without GAL4 expression. (**B**) *GMR81C04-Gal4* driving Flp recombinase allows EGFP::VGluT protein expression in FSB neurons, which are glutamatergic. No EGFP signal is detected when no GAL4 is expressed. (**C**) *GH146-GAL4* driving Flp recombination derepresses EGFP::VGAT protein expression in the APL neurons which are known to be GABAergic. No EGFP signal is detected without GAL4 expression. Dashed white lines indicate the brain outline. Scale bars = 20 μm.

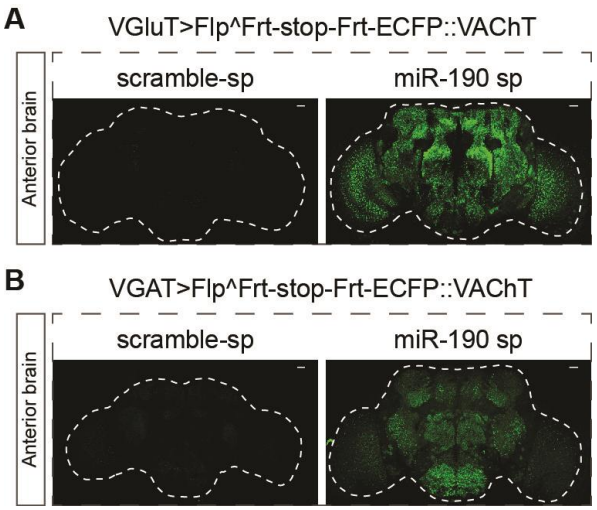

Figure S4. Suppression of miR-190 function allows VAChT protein expression in VGluT (A) and VGAT (B) positive neurons. Representative pictures show the anterior brain signals. Posterior brain stacks are shown in Fig. 2C-D. Dashed white lines indicate the outline of the brain. Scale bars = 20 µm.

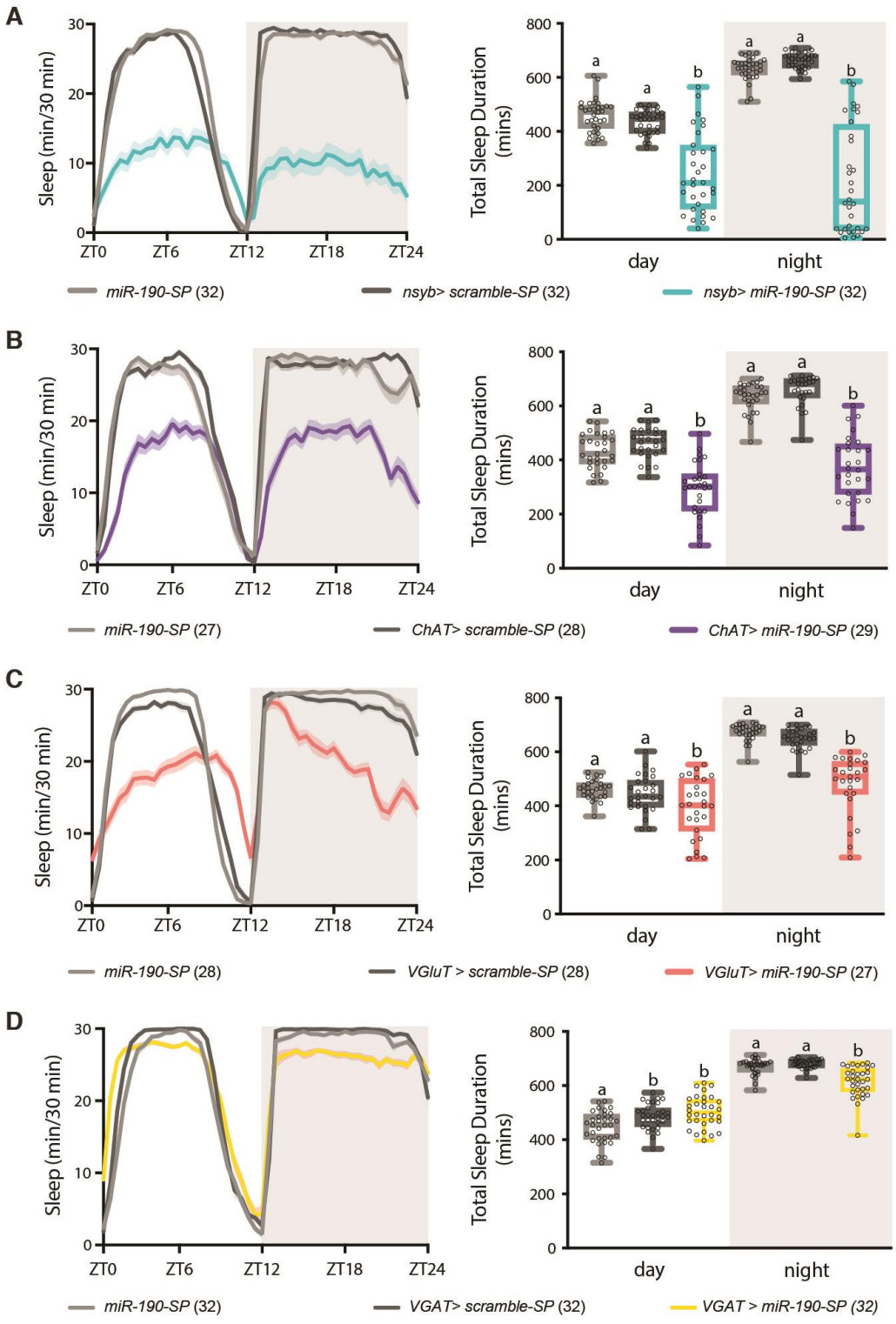

Figure S5. Suppression of miR-190 function reduces total sleep. (**A-D**) Left panels: sleep per 30 mins across 24 hours of a 12:12 light:dark cycle. Right panels: Quantification of total sleep duration when miR-190 function is suppressed in all neurons with *nsyb-Gal4*, a panneuronal

driver (**A**), cholinergic neurons with *ChAT-Gal4* (**B**), glutamatergic neurons with *VGluT-Gal4* (**C**), and GABAergic neurons with *VGAT-Gal4* (**D**). Data are shown as mean ± SEM, and gray circles show individual values. Statistical differences are indicated by letters, with genotypes that are not significantly different having the same letter. Data were analyzed with one-way ANOVA with Tukey's multiple comparisons test or Kruskal-Wallis with Dunn's multiple comparisons test (depending on data set structure), $p < 0.05$.

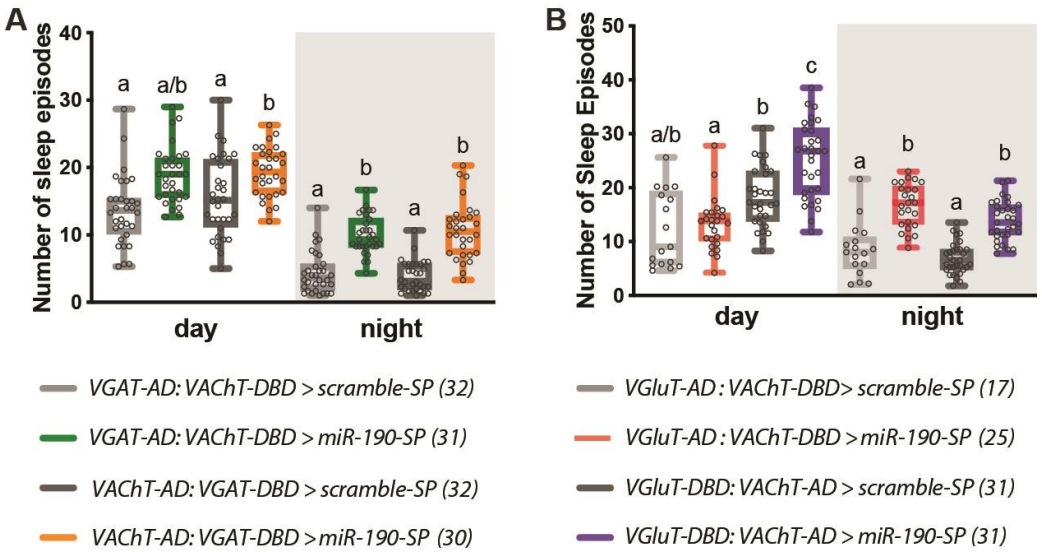

Figure S6. Suppression of miR-190 in GABA^{ACh} and Glu^{ACh} neurons with two independent split-Gal4s fragments sleep and increases the number of sleep episodes. Sleep fragmentation is characterized by both reduced sleep episode duration (as shown in Fig. 3BC) and by increased number of episodes. (**A**) MiR-190 suppression in GABA^{ACh} neurons increases sleep episodes number significantly. (**B**) MiR-190 suppression in Glu^{ACh} neurons makes the number of sleep episodes increase significantly during nighttime. Data are shown as mean ± SEM, and gray circles show individual values. Statistical differences are indicated by letters, with genotypes that are not significantly different having the same letter. Data were analyzed with one-way ANOVA with Tukey's multiple comparisons test or Kruskal-Wallis with Dunn's multiple comparisons test (depending on data set structure), $p < 0.05$.

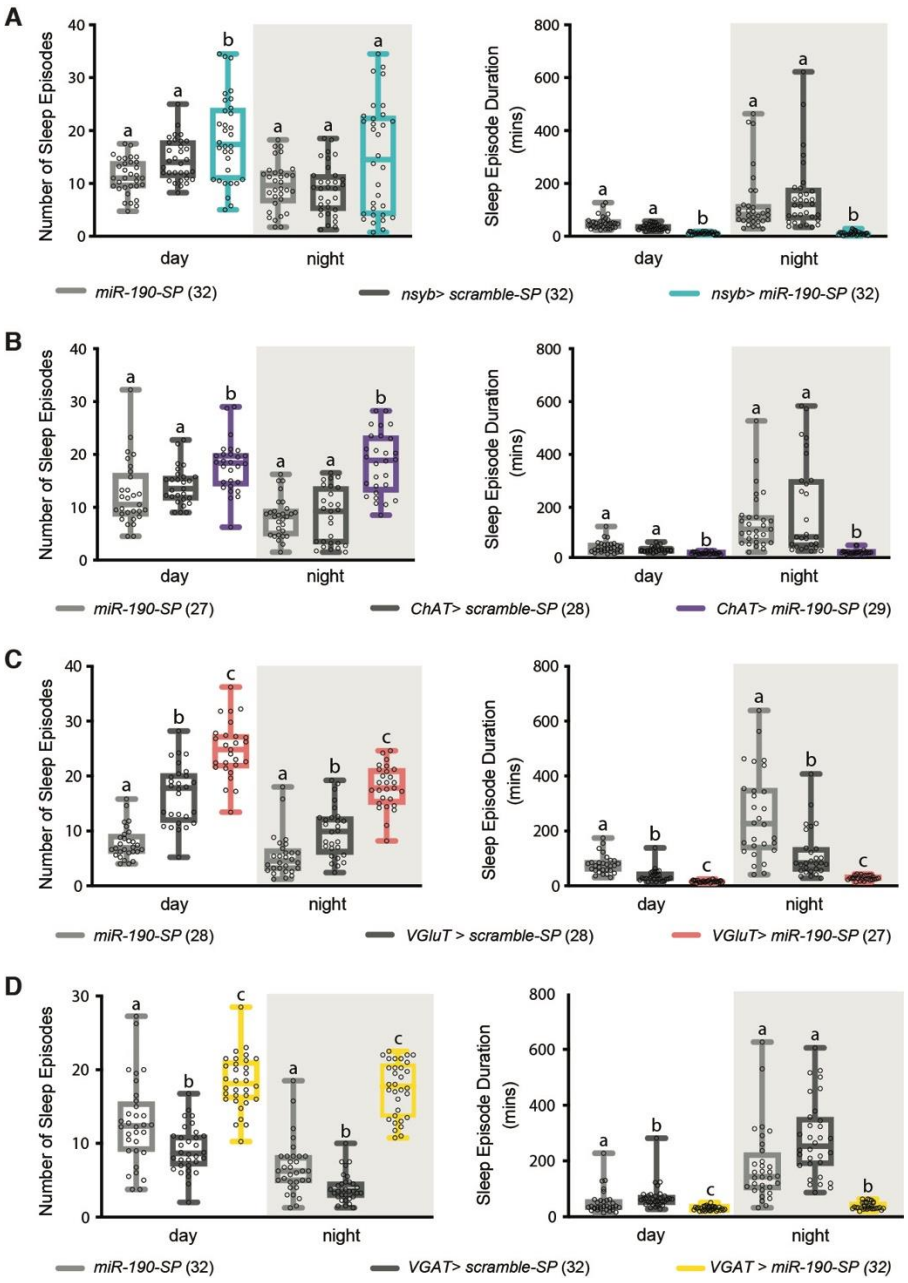

673

674 **Figure S7. Sleep fragmentation when miR-190 function is suppressed.** Quantification of
675 number of sleep episodes (left) and episode duration (right) when miR-190 function is
676 suppressed in all neurons with *nsyb-Gal4* a panneuronal driver (**A**), cholinergic neurons with
677 *ChAT-Gal4* (**B**), glutamatergic neurons with *VGluT-Gal4* (**C**), and GABAergic neurons with
678 *VGAT-Gal4* (**D**). Data are shown as mean ± SEM, and gray circles show individual values.
679 Statistical differences are indicated by letters, with genotypes that are not significantly different

680 having the same letter. Data were analyzed with one-way ANOVA with Tukey's multiple
681 comparisons test or Kruskal-Wallis with Dunn's multiple comparisons test (depending on data
682 set structure), $p < 0.05$.

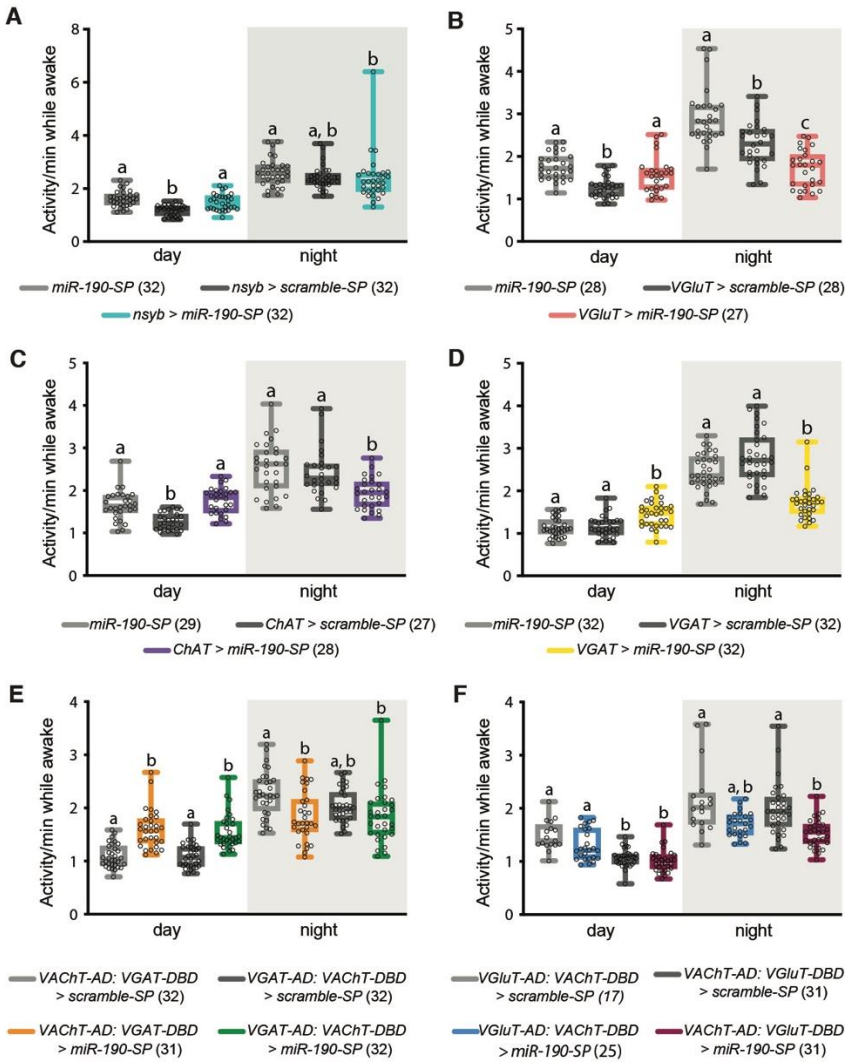

Figure S8. Activity while awake is either not affected or reduced when miR-190 function is suppressed. Quantification of activity while awake when miR-190 function is suppressed in all neurons with *nsyb-Gal4* a panneuronal driver (**A**), glutamatergic neurons with *VGluT-Gal4* (**B**), cholinergic neurons with *ChAT-Gal4* (**C**), GABAergic neurons with *VGAT-Gal4* (**D**), GABA^{ACh} neurons with two different split-Gal4s (**E**), and Glu^{ACh} neurons with two different split-Gal4 drivers (**F**). Data are shown as mean ± SEM, and gray circles show individual values. Statistical differences are indicated by letters, with genotypes that are not significantly different having the same letter. Data were analyzed with one-way ANOVA with Tukey's multiple comparisons test

692 or Kruskal-Wallis with Dunn's multiple comparisons test (depending on data set structure), $p <$

693 0.05.

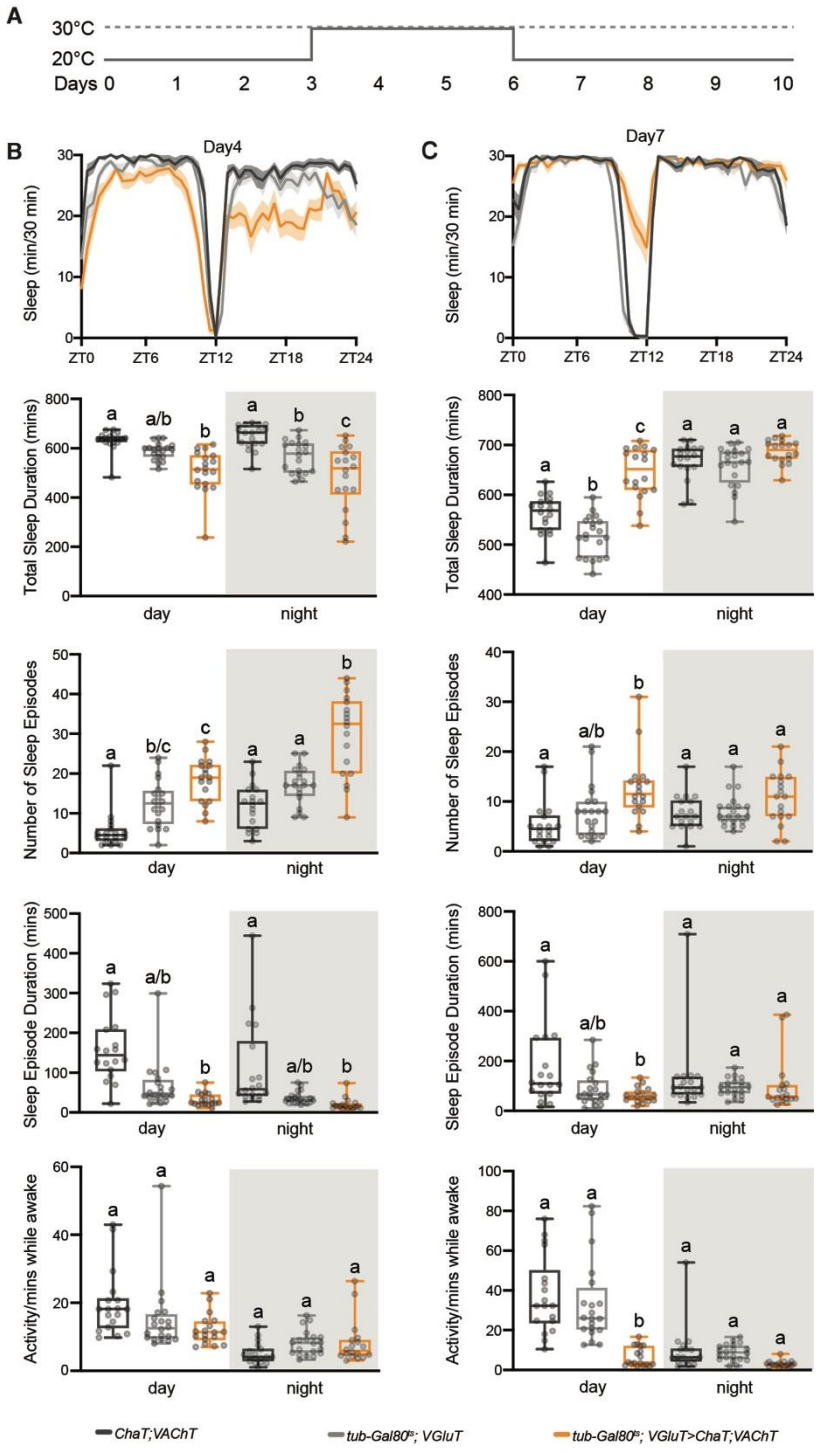

Figure S9. Overexpression of ChAT and VAChT in adult glutamatergic neurons decreases and fragments sleep. (**A**) Schematic diagram of temperature shift to 30 ℃ on day 4 and back to 20 ℃ on day 7. (**B**) Overexpression of ChAT and VAChT in glutamatergic neurons on day 4 decreases nighttime sleep significantly and increases the number of nighttime sleep episodes

699 significantly. (**C**) On day 7, daytime sleep rebounds significantly, overshooting basal levels,
700 though it is notable that there is a suppression of locomotor activity as well. Sleep structure
701 returns to normal. N=18-20. Data are shown as mean ± SEM, and gray circles show individual
702 values. Statistical differences are indicated by letters, with genotypes that are not significantly
703 different having the same letter. Data were analyzed with one-way ANOVA with Tukey's
704 multiple comparisons test or Kruskal-Wallis with Dunn's multiple comparisons test (depending
705 on data set structure), $p < 0.05$.

706

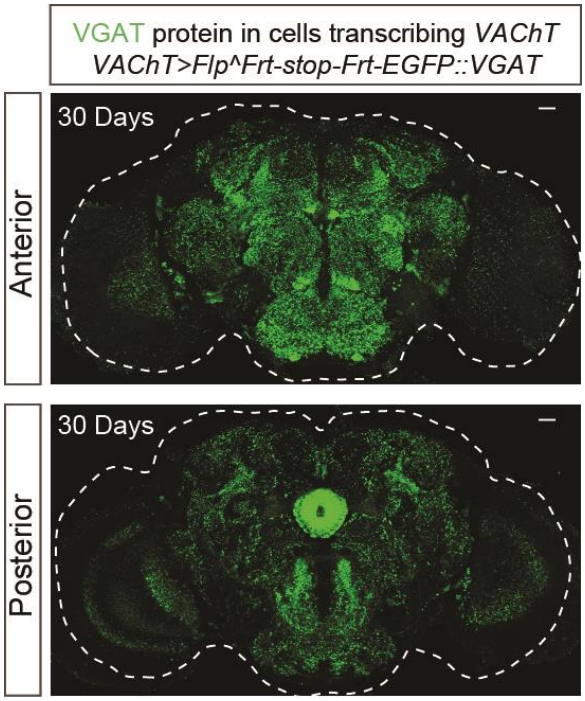

Figure S10. In 30 days aging flies, *VAChT-Gal4* flip-out derepression of *EGFP::VGAT* shows a pattern unchanged by age. Anterior pictures are shown in upper panel, with posterior pictures in lower panel. Young flies are shown for comparison in Fig. 1I. Scale bars = 20 µm.

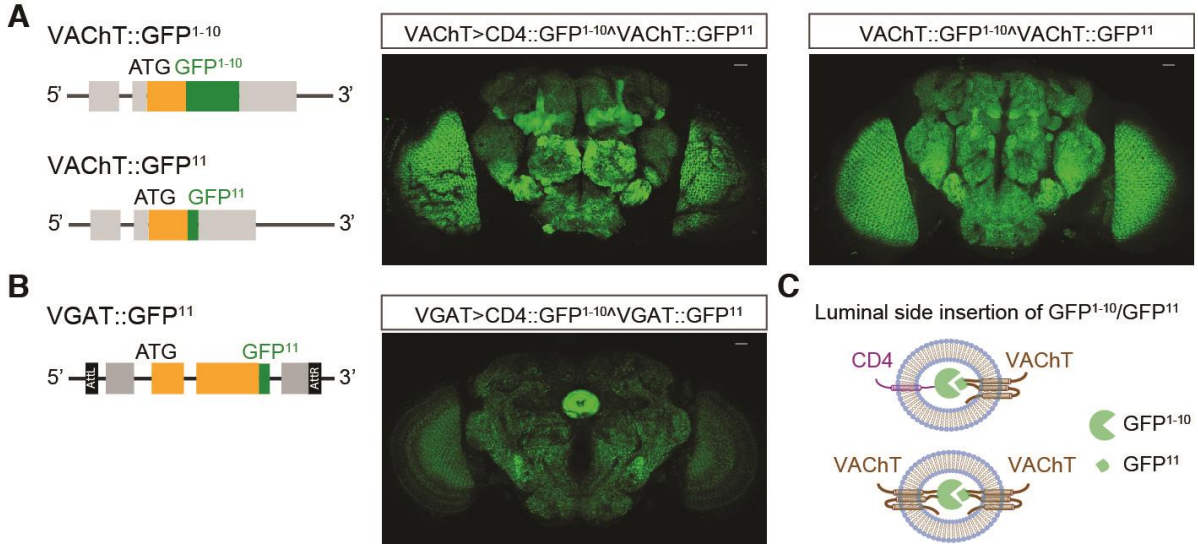

712

713 **Figure S11. *VAChT::GFP$^{1-10}$*, VAChT::GFP^{11} and VAChT::GFP^{11} display split Gal4 on the**
714 **luminal side of synaptic vesicles.** (**A**) Schematic diagrams in left panel show the *VAChT*
715 insertion sites for *GFP$^{1-10}$* and *GFP^{11}* used to create CRISPR alleles. These are predicted to be
716 lumenal (https://phobius.sbc.su.se/). To test this, we crossed *VAChT::GFP^{11}* with *VAChT>UAS-*
717 *CD4-GFP$^{1-10}$* which is known to be lumenal in vesicles. Strong GFP signal confirms GFP^{11} is
718 located on the luminal side. Crossing *VAChT::GFP$^{1-10}$* and *VAChT::GFP^{11}* also reconstitutes a
719 strong signal confirming that *VAChT::GFP$^{1-10}$* also displays on the luminal side. (**B**) Schematic
720 diagram in left panel shows the *VGAT* insertion site for *GFP^{11}*. Reconstituted GFP signal for
721 *VGAT>CD4-GFP$^{1-10}$* and *VGAT::GFP^{11}* indicate the VGAT-GFP^{11} displays on the luminal side.
722 (**C**) The cartoon shows the strategy: only when GFP$^{1-10}$ and GFP^{11} are located on the same side
723 of the vesicle membrane can GFP signal be reconstituted and detected. Scale bars = 20 μm.

724

725

726

Table S1.

Guide RNAs for VAChT, VGAT and VGluT lines.

VAChT-gRNA	GGGCCGACGCCTCCACCGTTG
VGAT-gRNA	GCGTTCTGGAATTTGCTGTC
VGluT-gRNA	GAAGGGTCTGACGGCGTTTA

Table S2.

Primers for S2 cell assay plasmids.

pAc5.1-Fluc-ChaT-3'UTR	Forward primer	GATCGCCGTGTAAGCGGCCGCTCGAGACG AACTAGACTAGAATGTC
	Reverse primer	GGCTTACCTTCGAAGGGCCCTCTAGAGGTT TGTAATGCATTTATTT
pAc5.1-Fluc-VAChT-3'UTR	Forward primer	GATCGCCGTGTAAGCGGCCGCTCGAGACT GTTGCCCCGAACAGATA
	Reverse primer	GGCTTACCTTCGAAGGGCCCTCTAGACCAT GGTTAACAATTATATT
pAc5.1-Fluc-ChaT-3'UTR-190-del	Forward primer Fragment 1	CGAACTAGACTAGAATGTCGCTAGGATTG GGGTCCACCAGAAAAAAAAAAAGTTAATG TACCTAAGCAGG
	Reverse primer Fragment 1	TACGAGGATACTTTGGTAACAAAGCGAAT GGGTTGCGTAT
	Forward primer Fragment 2	ATACGCAACCCATTCGCTTTGTTACCAAAG TATCCTCGTA
	Reverse primer Fragment 2	TGGGATGTATATAAATTTATATTGTTACGT CTCAAGTCTA
	Forward primer Fragment 3	TAGACTTGAGACGTAACAATATAAATTTA TATACATCCCA
	Reverse primer Fragment 3	GGCTTACCTTCGAAGGGCCCTCTAGAGGTT TGTAATGCATTTATTT
pAc5.1-Mir-190	Forward primer	GACCCCGGATCGGGGTACCTACTAGTCGA ACTAATTGATGGTTCCA
	Reverse primer	CCTTCGAAGGGCCCTCTAGACTCGAGGCG AGGGTCACAGTAATAAT
pAc5.1-Mir-scramble	Forward primer	CAGAGACCCCGGATCGGGGTACCTGGGCG TATAGACGTGTTACACCTCGAGTCTAGAG GGCCCTTCGA
	Reverse primer	TCGAAGGGCCCTCTAGACTCGAGGTGTAA CACGTCTATACGCCCAGGTACCCCGATCC GGGGTCTCTG

737 **Table S3.**
738 Fly genotypes for figures.
739

Figure	Genotype
Fig. 1B	VGluT::AD/+;VAChT::DBD/UAS-myrGFP-2A–RedStinger
Fig. 1C	VGAT::AD/+;VAChT::DBD/UAS-myrGFP-2A–RedStinger
Fig. 1D:Left to right	VGAT::AD/+;VAChT::DBD/UAS-UNC84::GFP
	VGluT::AD/+;VAChT::DBD/UAS-UNC84::GFP
Fig. 1I:Left to right	UAS-Flp, Frt-stop-Frt-EGFP::VGluT/+; VAChT-Gal4/+
	UAS-Flp/VGluT-Gal4;Frt-stop-Frt-ECFP::VAChT/+
	UAS-Flp, Frt-stop-Frt-EGFP::VGAT/+; VAChT-Gal4/+
	UAS-Flp/VGAT-Gal4; Frt-stop-Frt-ECFP::VAChT/+
Fig. 2C:Left to right	UAS-Flp/VGluT-Gal4; Frt-stop-Frt-ECFP::VAChT/UAS-scramble-SP
	UAS-Flp/VGluT-Gal4;Frt-stop-Frt-ECFP::VAChT/UAS-miR-190-SP
Fig. 2D:Left to right	UAS-Flp/VGAT-Gal4;Frt-stop-Frt-ECFP::VAChT/UAS-scramble-SP
	UAS-Flp/VGAT-Gal4; Frt-stop-Frt-ECFP::VAChT/UAS-miR-190-SP
Fig. 2E:Left to right	UAS-Flp,Frt-stop-Frt-EGFP::VGluT/+; VAChT-Gal4/UAS-scramble-SP
	UAS-Flp,Frt-stop-Frt-EGFP::VGluT/+; VAChT-Gal4/UAS-miR-190-SP
Fig. 2F:Left to right	UAS-Flp, Frt-stop-Frt-EGFP::VGAT/+; VAChT-Gal4/UAS-scramble-SP
	UAS-Flp, Frt-stop-Frt-EGFP::VGAT/+; VAChT-Gal4/UAS-miR-190-SP
Fig. 4B	Frt-stop-Frt-EGFP::VGluT/+; Flp-VAChT-3'UTR/+
Fig. 4C	Frt-stop-Frt-EGFP::VGAT/+; Flp-VAChT-3'UTR/+
Fig. 4D	UAS-Flp/VGAT-Gal4; Frt-stop-Frt-ECFP::VAChT/+
Fig. 4E	VGAT::GFP^{11}/+;VAChT::GFP$^{1-10}$/+
Fig. S1B:Left to right	VAChT-Gal4/UAS-myrGFP-2A–RedStinger
	VGluT-Gal4/+; UAS-myrGFP-2A–RedStinger/+
	VGAT-Gal4/+; UAS-myrGFP-2A–RedStinger/+
Fig. S1C	VGluT::DBD/+; VAChT::AD/UAS-myrGFP-2A–RedStinger
Fig. S1D	VGAT::DBD/+; VAChT-AD/UAS-myrGFP-2A–RedStinger
Fig. S3A:Left to right	UAS-Flp/+;Frt-stop-Frt-ECFP::VAChT/+
	UAS-Flp/+; VT030559-Gal4/Frt-stop-Frt-ECFP::VAChT
Fig. S3B:Left to right	UAS-Flp, Frt-stop-Frt-EGFP::VGluT/+
	UAS-Flp, Frt-stop-Frt-EGFP::VGluT/+; GMR81C04-Gal4/+
Fig. S3C:Left to right	UAS-Flp, Frt-stop-Frt-EGFP::VGAT/+
	UAS-Flp,Frt-stop-Frt-EGFP::VGAT/GH146-Gal4
Fig. S4A:Left to right	UAS-Flp/VGluT-Gal4; Frt-stop-Frt-ECFP::VAChT/UAS-scramble-SP
	UAS-Flp/VGluT-Gal4; Frt-stop-Frt-ECFP::VAChT/UAS-miR-190-SP
Fig. S4B:Left to right	UAS-Flp/VGAT-Gal4; Frt-stop-Frt-ECFP::VAChT/UAS-scramble-SP
	UAS-Flp/VGAT-Gal4; Frt-stop-Frt-ECFP::VAChT/UAS-miR-190-SP

Fig. S10:Left to right	UAS-Flp, Frt-stop-Frt-EGFP::VGluT/+; VAChT-Gal4/+
	UAS-Flp, Frt-stop-Frt-EGFP::VGAT/+; VAChT-Gal4/+
Fig.S11A:Left to right	UAS-CD4-GFP$^{1-10}$,VAChT-GFP$^{11/}$VAChT-Gal4
	VAChT-GFP$^{1-10}$/VAChT-GFP^{11}
Fig. S11B	VGAT-Gal4/VAChT-GFP^{11}; UAS-CD4-GFP$^{1-10}$/+

740

741

Data S1.

Plasmids maps.